Drift hole structure and dynamics with turbulence driven flows

Y. Kosuga[1,2,a)] and P. H. Diamond[1,2]

[1]*Center for Astrophysics and Space Sciences and Center for Momentum Transport and Flow Organization, University of California at San Diego, La Jolla, California 92093, USA*
[2]*WCI Center for Fusion Theory, National Fusion Research Institute, Gwahangno 113, Yusung-gu, Daejeon 305-333, Korea*

The role of turbulence driven flows in describing drift hole structure and dynamics is discussed. Turbulence driven flows enter the plasma medium response and alter drift hole structures by changing the screening length of the drift hole potential. Specifically, turbulence driven flows shift the drift hole potential radially, and absorb drift hole energy via the hole-flow resonance. It is shown that the absorption shifts the phase of a momentum flux, and so enables the irreversible coupling of drift holes to turbulence driven flows. We show that drift holes and turbulence driven flows are dynamically coupled, and self-regulate each other, so that a stationary state can be achieved with non-zero turbulence driven flows. As an application, a bound on the fluctuation amplitude in the coupled system is derived. The bound is obtained by requiring that the resultant zonal flow velocity should be smaller than the critical flow velocity for the drift hole potential to be self-bound (i.e., the velocity that the screening length be positive). The result predicts $|\tilde{\phi}|^2_{max} \sim (\nu_d/\omega_{ci})(k_\parallel/k_y)$, where zonal flow damping appears as a control parameter. The implications of this result for the problem of edge-core coupling (i.e., explaining turbulence and transport in "No Man's Land") are discussed. © 2012 American Institute of Physics. [http://dx.doi.org/10.1063/1.4737197]

I. INTRODUCTION

A coherent structure is a frequently observed element in turbulent systems. While a coherent structure often forms in fluid turbulence in *real space*, such structure also forms in *phase space*. In real space, a well-known example of such a coherent structure is a coherent vortex in fluid turbulence, especially one observed in quasi-2D fluids, including an "eye" on Jupiter. Another example of real space structures is a density blob or hole in tokamak plasmas[1,2] (Fig. 1). A density blob or hole is generated at the plasma edge, where strong gradient perturbations generate an outgoing blob and an incoming hole. Once generated, the density hole (blob) can grow as it climbs (descends) the density gradient. This observation suggests that such incoming nonlinear structures, as well as linear instabilities driven by local gradients, can stir turbulence and enhance fluctuation levels. In particular, such structure driven turbulence may play a role in understanding the phenomenology of "No Man's Land" in tokamak plasmas, a region that connects the tokamak core and edge.

A coherent structure in turbulence and its growth are not only limited to real space, but also extend to phase space. The simplest example of such structures is that from 1D Vlasov plasmas, such as a Bernstein-Greene-Kruskal (BGK) vortex,[3] a phase space density hole,[4] and clump-hole pairs[5] in the context of the Berk-Breizman model[5] for energetic particle phenomenology. These coherent structures in phase space form due to strong wave-particle resonance, which generates a potential that can hold particles together in a trough. These trapped particles in turn generate a self-potential, leading to formation of a self-sustained structure. Once formed, such

structures can grow by extracting free energy, as depicted in Fig. 1. More precisely, the growth is made possible by momentum exchange with, and velocity scattering by other species[4] (for example, structures in ions must scatter electrons to maintain the quasi-neutrality). Such mechanisms allow a hole to be displaced up the phase space density gradient. The displacement leads to the growth of the hole, since phase space density is necessarily conserved along trajectory. Such growth of phase space density structures was predicted theoretically[4,6] and confirmed in numerical simulations.[5,7–10] One of the striking features of the growth is that it can be subcritical, namely structures can extract free energy even when plasmas are predicted to be linearly stable.[6] Based on this, the fundamental role of linear stability theory was called into question.[6]

A coherent structure in phase space also forms in more complex systems, such as inhomogeneous magnetized plasmas, a system of interest to the fusion community. Earlier study showed that BGK solutions can be obtained in such a system and thus a phase space density hole (dubbed drift hole[11]) forms. Due to the magnetic field, the drift hole has distinctive features in the parallel and the perpendicular directions. In the parallel direction, the structure is similar to the 1D Vlasov case, where trapping is provided by a potential field. In contrast, the drift hole has a perpendicular structure which can be viewed as a localized $E \times B$ vortex. Once formed, as with other phase space structures, drift holes can drive subcritical instability. As for the 1D Vlasov plasma, this is a consequence of the conservation of total phase space density, which necessitates that a localized depletion grows as it is displaced up the gradient (Fig. 1). However, unlike the 1D problem, drift hole dynamics necessitates a spatial flux of particles. For example, motion of an electron drift

a)Electronic mail: yukosuga@physics.ucsd.edu.
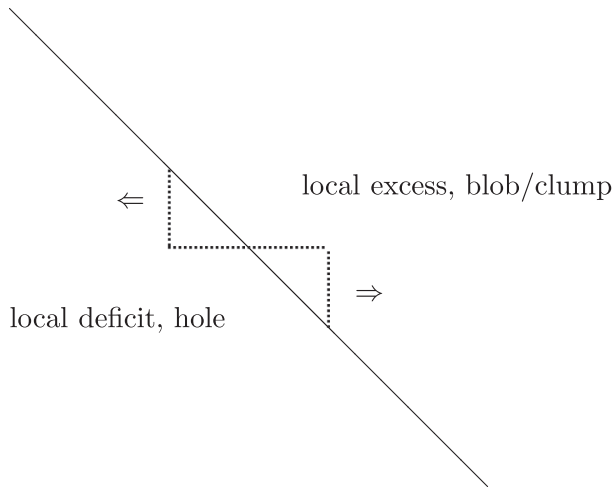
FIG. 1. Formation and growth of structures. The flattening of the gradient leads to the formation of blobs (local excess) and holes (local deficit). Once formed, holes (blobs/clumps) can grow by propagating against (down) the gradient.

FIG. 2. Growth of drift hole and zonal flow.

hole necessitates a spatial flux of ions. Intuitively, the displacement and the growth process of the electron drift hole may be understood in terms of its screening field. Namely, once the electron drift hole forms, it attracts a cloud of screening field. The screening field can spatially scatter ions, which forces the electron drift hole to move up the gradient, so as to satisfy the quasi-neutrality condition.

While early studies examined the basic structure and dynamics of drift holes, further development is still necessary. This is especially true regarding the issue of zonal flows.[12] The coupling of zonal flows in drift hole physics can be motivated from an analogy to dynamics of *drift wave* turbulence. It has been demonstrated that zonal flows have significant impact on fluctuation dynamics of drift wave turbulence via amplitude suppression and cross phase decorrelation.[12] This naturally leads us to the expectation that zonal flows could also impact *drift hole* driven relaxation processes. However, such zonal flow coupling was ignored in an earlier study.[11] This is partly because that study naively ignored mesoscales and envelope scales, and so treated $\langle \tilde{v}_x \nabla_\perp^2 \tilde{\phi} \rangle \sim \mathrm{Re} i k_y k_\perp^2 |\tilde{\phi}|_k^2 \to 0$. Note that the polarization charge flux is equivalent to the Reynolds force via the Taylor identity[13–15] $\langle \tilde{v}_x \nabla_\perp^2 \tilde{\phi} \rangle \sim \partial_x \langle \tilde{v}_x \tilde{v}_y \rangle$.

The role of polarization charge flux in zonal flow coupling may be further clarified in the context of potential vorticity (PV) dynamics in the quasi-geostrophic (QG) system. The important physical meaning of the conservative PV dynamics is the conservation of a total charge.[14,16] For example, in Hasegawa-Wakatani system,[17] the PV is $q = n_e - \rho_s^2 \nabla_\perp^2 \phi$, where the total charge q consists of (guiding center) electron charge and polarization charge. The growth of the PV fluctuation is driven by transport of the total q. Since the transport of the total q contains polarization charge flux, and since the polarization charge flux is equivalent to Reynolds force,[13–15] growth of fluctuation in the QG system *must* involve zonal flow acceleration. The point is depicted in Fig. 2. Such coupled evolution was formulated as a momentum theorem[13,14,18] for the PV fluctuation and zonal flow. Similarly, in the drift hole dynamics,
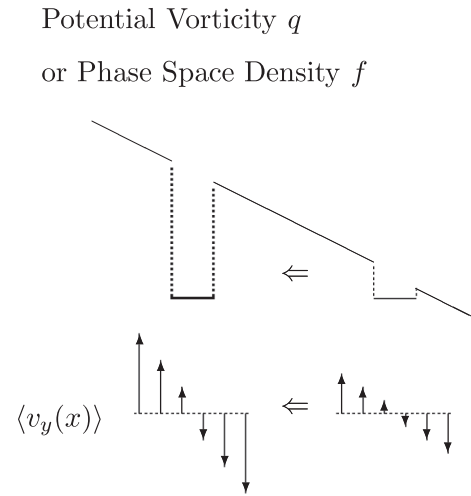
phase space density f is related to a total charge via $\int d^3v f_e = \int d^3v f_i^{GC} + \rho_s^2 \nabla_\perp^2 \phi$. Total charge conservation (or the quasi-neutrality constraint) requires the screening cloud of a structure to scatter the oppositely charged particles, as well as polarization charge, during the growth process. Thus, we expect that the growth of the drift hole structure be accompanied by zonal flow growth, as for PV dynamics in Hasegawa-Wakatani system.

In this paper, we present the theory of the structure and dynamics of drift holes with turbulence driven flows. Simply, drift hole structures are influenced by flows, since flows alter the medium response. The effect shows up in the screening length of the self-consistent drift hole potential. The flow correction in the screening leads to the shift of the $E \times B$ vortex produced by drift hole potential, analogous to a well known shear flow effect[19] on eigenmode structure.[20] In addition, the drift hole is coupled to flows via hole-flow resonance, which provides the proper phase for non-zero polarization charge flux and hence Reynolds force. The non-zero flow coupling has an impact on drift hole dynamics as well. To access free energy and to grow, (electron) drift holes must move up the gradient by scattering guiding center ions, while the structure is coupled to zonal flows via the polarization charge flux. It is shown that drift hole growth is coupled to turbulence flow generation. The coupled dynamics of drift holes and zonal flows is analogous to that of drift wave-zonal flow turbulence,[12,21] in which waves and flows regulate one another. Since drift hole and zonal flow are coupled together, a stationary state with a finite zonal flow is possible. We argue that since even a single phase space structure can drive zonal flows, familiar concepts for zonal flow generation such as inverse cascade,[22] Rhine's scale,[23] and modulational instability,[12] etc., are maybe useful but are *not* fundamental. We also discuss the implication for the saturated amplitude of the drift hole. Since the drift hole and zonal flow are coupled, a non-zero zonal flow can result in a stationary state. The resultant zonal flow in turn deforms the drift hole structure itself by modifying the screening effect. By requiring that *potential screening* is *finite* in the presence of the stationary zonal flow, an upper bound on drift hole

amplitude in the drift hole-zonal flow system is calculated. The result indicates $|\phi|^2_{max} \sim (\nu_d/\omega_{ci})(k_\parallel/k_y)$, where the zonal flow damping appears as a control parameter.

The implication for the edge-core connection problem—the "No Man's Land" phenomenology—is discussed as well. It has long been known that a strong perturbation at the tokamak edge can nucleate localized quasi-coherent structures (blobs and holes).[1,2] Once formed, such holes can propagate inward and bombard the" "No Man's Land" region. Since such structures will also tap free energy in a different way from linear instabilities driven by the local gradients, these structures can enhance the turbulence level in the "No Man's Land" region. This is a potentially important step toward resolving the long standing problem of reconciling drift turbulence theories with observed levels of fluctuations and transport near the edge of the plasma.

The remainder of the paper is organized as follows. In Sec. II, the radial structure of the drift hole potential is discussed in detail. The drift hole potential is determined in the plasma medium with flows. In Sec. III, we show that drift hole growth is coupled to turbulence driven flows. The saturation dynamics is discussed as well, along with the calculation of an upper bound on the fluctuation amplitude at saturation. Section IV presents the discussion and conclusion.

II. DRIFT HOLE STRUCTURE WITH FLOWS

Here, we construct the drift hole potential and discuss its radial structure with flows in detail. Generally speaking, a drift hole will form at a strong resonance, which traps charged particles in a potential structure. In turn, the trapped charges produce a self-potential to reinforce the self-binding. Specifically, the drift hole has distinct structure both in the parallel and perpendicular directions. In the parallel direction, drift hole structure is characterized by trapping, and thus is similar to the 1D problem. In contrast, in the perpendicular direction, the structure can be viewed as a $E \times B$ vortex. Mathematically, drift holes are BGK solutions of magnetized plasmas, which are constructed by solving both the kinetic and Poisson equations to determine the particle distribution and potential, self-consistently.

Assuming electron trapping here for definiteness, self-consistent potential is determined by solving the gyrokinetic (GK) Poisson equation[11,24,25]

$$\frac{|e|\phi}{T_e} + \int_t dv_\parallel \{f^t_e(\phi) - \langle f_e \rangle\} = -(\partial_t + \langle v_y \rangle \partial_y)^{-1} v_{*e} \frac{\partial}{\partial y} \frac{|e|\phi}{T_e}$$
$$+ \rho^2_s \nabla^2_\perp \frac{|e|\phi}{T_e}. \quad (1)$$

Here, the lefthand side (electrons) consists of the screening by adiabatic electrons and the trapped electrons (hole). The righthand side (ions) contains the screening ions, including the guiding center ions with flows and the polarization ions. We can rewrite Eq. (1) in a form where the screening effect is more apparent

$$\left(\partial^2_x - \hat{\lambda}^{-2}\right)\frac{e\phi}{T_e} = \frac{1}{\rho^2_s}\int_t dv_\parallel \{f^t_e(\phi) - \langle f_e \rangle\}. \quad (2)$$

Here we introduced the screening length $\hat{\lambda}^{-2} \equiv \rho^{-2}_s \hat{\chi}$ and $\hat{\chi}$ is the susceptibility defined as

$$\hat{\chi} \equiv 1 - \rho^2_s \partial^2_y + (\partial_t + \langle v_y \rangle \partial_y)^{-1} v_{*e} \frac{\partial}{\partial y}. \quad (3)$$

Eq. (2) takes the form of Poisson equation to determine the potential, with the source from the trapped electrons and the screening from the untrapped charges. Here, the screening appears as an effect of the shielding medium, which consists of the adiabatic electrons, the guiding center ions with flows, and the polarization charges. Loosely, structure corresponds to a localized potential $\phi \sim \exp(-x/\lambda)$, which requires $\lambda^{-2} > 0$. If $\lambda^{-2} < 0$, the potential is not localized and $\phi \sim \exp(ik_x x)$, which may be viewed as symptomatic of Cerenkov radiation of energy. If $\phi \sim \exp(ik_x x)$ then a localized structure does not form. We hereafter focus on the former case of the localized potential, $\phi \sim \exp(-x/\lambda)$.

To solve Eq. (2), we need to specify f^t_e. f^t_e is obtained as a stationary solution for the drift kinetic equation

$$\partial_t f^t_e + v_\parallel \nabla_\parallel f^t_e + \frac{c}{B}\hat{z} \times \nabla\phi \cdot \nabla f^t_e - \frac{|e|}{m_e}E_\parallel \frac{\partial f^t_e}{\partial v_\parallel} = 0. \quad (4)$$

Eq. (4) has a stationary solution with the form $f^t_e[m_e v^2_\parallel/2 - |e|\phi]$. The solution of Eq. (2) obtained for any $f^t_e[m_e v^2_\parallel/2 - |e|\phi]$ is the BGK solution for magnetized plasmas. As a subclass of such BGK solutions, hole solutions are constructed by maximizing entropy. The form of f^t_e which maximizes the entropy of system is derived by Dupree,[4] and is

$$f^t_e = \langle f_e \rangle \exp\left(\frac{E + |e|\phi_m}{\tau}\right). \quad (5)$$

Here $E \equiv m_e v^2_\parallel/2 - |e|\phi$ is the total energy of the electrons, $-|e|\phi < E < -|e|\phi_m$ for electrons trapped in the electrostatic potential, and τ is a temperature used as the Lagrange multiplier to maximize entropy.[4] f^t_e is called the Maxwell-Boltzman hole. The potential for the Maxwell-Boltzmann hole is obtained by substituting f^t_e in Eq. (2) with the Maxwell-Boltzmann hole, and by then solving the resultant equation

$$\left(\partial^2_x - \hat{\lambda}^{-2}\right)\frac{e\phi}{T_e} = \frac{2}{\rho^2_s}\int^{-|e|\phi}_{-|e|\phi_m} \frac{dE}{\sqrt{2m_e(E + |e|\phi)}}\langle f_e \rangle$$
$$\times \left(\exp\left(\frac{E + |e|\phi_m}{\tau}\right) - 1\right). \quad (6)$$

Although in principle the potential for the Maxwell-Boltzmann hole is obtained by solving Eq. (6), we note that Eq. (6) is a nonlinear integro-differential equation which cannot be solved except for special cases. Leaving the discussion of the exact solution for the special case to the appendix, we consider an approximate solution for Eq. (6) below. A useful approximation to the Maxwell-Boltzmann hole is given by the box hole[4,11] (Figs. 3 and 4)
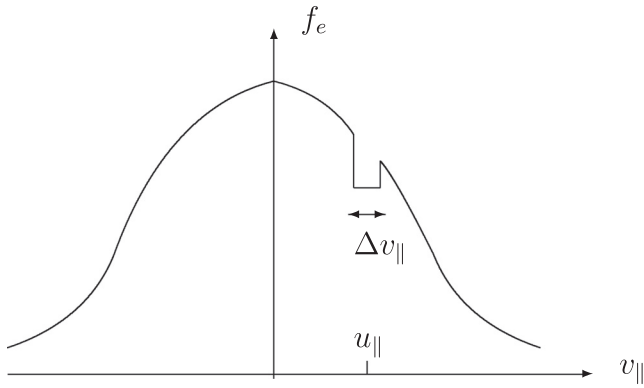
FIG. 3. Hole in velocity space.

$$f_e^t = \begin{cases} \langle f_e \rangle + f_H & \text{for} \begin{cases} |v_\parallel - u_\parallel| < \Delta v_\parallel/2 \\ |x| < \Delta x/2,\ |y| < \Delta y/2 \end{cases} \\ \langle f_e \rangle & \text{for others.} \end{cases} \quad (7)$$

Namely, the electrons trapped in the parallel direction consist of those moving at the speed $u_\parallel$, within a range of velocities width $\Delta v_\parallel$. Electrons are localized in the perpendicular plane as well, within a spatial region of extent Δx and Δy, forming a $E \times B$ vortex. As discussed before, the box hole is a reasonable approximation to the Maxwell-Boltzmann hole,[4,11] in particular, for $(E + |e|\phi_m)/\tau \ll 1$. For the box hole, the GK Poisson equation is

$$\left(\partial_x^2 - \hat\lambda^{-2}\right)\frac{e\phi}{T_e} = \frac{1}{\rho_s^2} f_H \Delta v_\parallel. \quad (8)$$

In the Fourier representation,

$$\left(\partial_x^2 - \lambda_k^{-2}[\langle v_y \rangle]\right)\frac{e\phi_k}{T_e} = \frac{1}{\rho_s^2} f_H \Delta v_\parallel \frac{\Delta y}{L_y} \frac{2}{k_y \Delta y} \sin\frac{k_y \Delta y}{2}. \quad (9)$$

Here L_y is the Fourier box size, $\lambda_k^{-2} = \rho_s^{-2}\chi(\mathbf{k}, k_\parallel u_\parallel)$, $\chi(\mathbf{k}, \omega) = 1 + k_y^2\rho_s^2 - \omega_{*e}/(\omega - k_y\langle v_y \rangle)$, and ω is evaluated at the hole Doppler frequency $\omega = k_\parallel u_\parallel$.
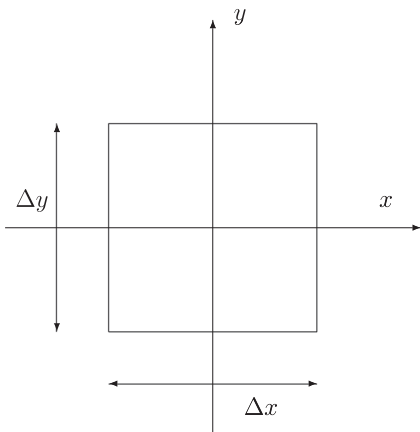
FIG. 4. Box hole.

Eq. (9) retains flow effects via the screening length or the susceptibility, $\lambda_k^{-2} \propto \chi$. Since the flow enters the susceptibility in the form $(k_\parallel u_\parallel - k_y\langle v_y \rangle)^{-1}$, it naturally raises the question of the singularity, or more physically, of the meaning and impact of the resonance between drift hole and shear flow. To treat the resonance properly, we employ the Plemelj formula,

$$\frac{1}{k_\parallel u_\parallel - k_y\langle v_y \rangle} = P\frac{1}{k_\parallel u_\parallel - k_y\langle v_y \rangle} - i\pi\delta(k_\parallel u_\parallel - k_y\langle v_y \rangle). \quad (10)$$

Here, the "P" denotes the principal value of the integral. We note that, of course, the formula makes sense only when it appears inside an integral, such as that arises in solving Eq. (9). Now, given the formula, the susceptibility becomes

$$\chi(\mathbf{k}, k_\parallel u_\parallel, \langle v_y \rangle) = 1 + k_y^2\rho_s^2 - P\frac{\omega_{*e}}{k_\parallel u_\parallel - k_y\langle v_y \rangle}$$
$$+ i\omega_{*e}\pi\delta(k_\parallel u_\parallel - k_y\langle v_y \rangle), \quad (11)$$

$$\cong \chi^{(0)}(\mathbf{k}, k_\parallel u_\parallel) - \left(\frac{k_y c_s}{k_\parallel u_\parallel}\right)^2 \frac{\langle v_y \rangle}{c_s}$$
$$+ i\omega_{*e}\pi\delta(k_\parallel u_\parallel - k_y\langle v_y \rangle), \quad (12)$$

where in the second line we assumed $k_\parallel u_\parallel > k_y\langle v_y \rangle$ and $\chi^{(0)}(\mathbf{k}, k_\parallel u_\parallel) \equiv 1 + k_y^2\rho_s^2 - \omega_{*e}/(k_\parallel u_\parallel)$ is the susceptibility without flow. Thus, flow modifies the plasma response via the susceptibility, which changes the screening of the drift hole potential. Alternatively put, flow determines the structure and dynamics of the screening cloud of trapped particles. Finally, the flow-hole resonance gives an absorption mechanism, namely $\mathrm{Im}\chi \propto \delta(k_\parallel u_\parallel - k_y\langle v_y \rangle)$. The resonance allows the flow to absorb the energy in the screening field. As a consequence of the resonance process, "cat's eye" patterns[26] are produced around the resonance location.

Having discussed the role of flow in plasma response, now we discuss the solution of Eq. (9). A general solution of Eq. (9) can be obtained as

$$\frac{|e|\phi_k}{T_e} = \int \frac{dx'}{\rho_s^2} G_k(x, x') f_H(x')\Delta v_\parallel \frac{\Delta y}{L_y} \frac{2}{k_y\Delta y}\sin\frac{k_y\Delta y}{2}, \quad (13)$$

where $G_k(x, x')$ is the Green's function which satisfies

$$(\partial_x^2 - \lambda_k^{-2}[\langle v_y \rangle])G_k(x - x') = \delta(x - x'). \quad (14)$$

Note the Green's function here may be viewed as a renormalized propagator which includes the effect of flow in the medium. However, while the physical interpretation is clear, it is not an easy task to obtain the full renormalized $G_k(x, x')$, due to the flow dependence in the screening length.

Thus, here we seek an approximate approach to obtain a solution ϕ_k. (As explained later, the approximation is analogous to the Born approximation in quantum mechanics.[27]) Namely, rather than keeping the flow in the screening term, we rewrite Eq. (9) as

$$(\partial_x^2 - \lambda_k^{(0)-2})\frac{e\phi_k}{T_e} = \frac{1}{\rho_s^2}f_H\Delta v_\parallel \frac{\Delta y}{L_y}\frac{2}{k_y\Delta y}\sin\frac{k_y\Delta y}{2}$$
$$+\left(\frac{k_yc_s}{k_\parallel u_\parallel}\right)^2\frac{\langle v_y\rangle}{c_s}\frac{|e|\phi_k}{T_e}$$
$$-i\omega_{*e}\pi\delta(k_\parallel u_\parallel - k_y\langle v_y\rangle)\frac{|e|\phi_k}{T_e}, \quad (15)$$

to obtain

$$\frac{|e|\phi_k}{T_e} = \int\frac{dx'}{\rho_s^2}G_k^{(0)}(x,x')f_H(x')\Delta v_\parallel\frac{\Delta y}{L_y}\frac{2}{k_y\Delta y}\sin\frac{k_y\Delta y}{2}$$
$$+\int\frac{dx'}{\rho_s^2}G_k^{(0)}(x,x')\left(\frac{k_yc_s}{k_\parallel u_\parallel}\right)^2\frac{\langle v_y(x')\rangle}{c_s}\frac{|e|\phi_k(x')}{T_e}$$
$$-\int\frac{dx'}{\rho_s^2}G_k^{(0)}(x,x')i\omega_{*e}\pi\delta$$
$$\times(k_\parallel u_\parallel - k_y\langle v_y(x')\rangle)\frac{|e|\phi_k(x')}{T_e}. \quad (16)$$

Here $G_k^{(0)}(x,x')$ is the "bare" Green's function, which satisfies

$$(\partial_x^2 - \lambda_k^{(0)-2})G_k^{(0)}(x,x') = \delta(x-x'), \quad (17)$$

and thus

$$G_k^{(0)}(x,x') = -\frac{\lambda_k^{(0)}}{2}\exp\left(-\frac{|x-x'|}{\lambda_k^{(0)}}\right). \quad (18)$$

Simply put, the first term in Eq. (16) describes an isotropic $E\times B$ vortex, the second term describes a shift to the isotropic $E\times B$ vortex, and the third term accounts for flow-hole resonance and contributes to a non-zero momentum flux. We consider each term in detail in the following.

The first term in Eq. (16) describes an isotropic $E\times B$ vortex, which was obtained in an earlier study.[11] The solution is

$$\frac{e\phi_k^{(0)}}{T_e} = -\frac{\Delta v_\parallel f_H}{\chi}\frac{\Delta y}{L_y}\frac{2}{k_y\Delta y}\sin\left(\frac{k_y\Delta y}{2}\right)X_k^{(0)}(x), \quad (19)$$

where $X_k^{(0)}(x)$ is a function which determines the radial profile of the potential field

$$X_k^{(0)}(x) = \begin{cases} \exp\left(-\frac{|x|}{\lambda_k}\right)\sinh\left(\frac{\Delta x}{2\lambda_k}\right) & \text{for } |x| > \Delta x/2 \\ 1 - \cosh\left(\frac{x}{\lambda_k}\right)\exp\left(-\frac{\Delta x}{2\lambda_k}\right) & \text{for } |x| < \Delta x/2. \end{cases}$$
$$(20)$$

Hereafter it is understood that the susceptibility and the screening length are evaluated without flow, $\lambda_k^{-2} = \rho_s^{-2}\chi$ and $\chi = 1 + k_y^2\rho_s^2 - \omega_{*e}/(k_\parallel u_\parallel) > 0$. The potential (Eq. (19)) is given by $\phi = \sum_{k_y}\phi_k\exp(ik_yy)$ and plotted in Fig. 5; the drift hole potential leads to a localized, $E\times B$ vortex in 2D (x,y) plane.

Here, in contrast, we have the two additional terms in Eq. (16) due to the flow effects. Physically, as discussed in
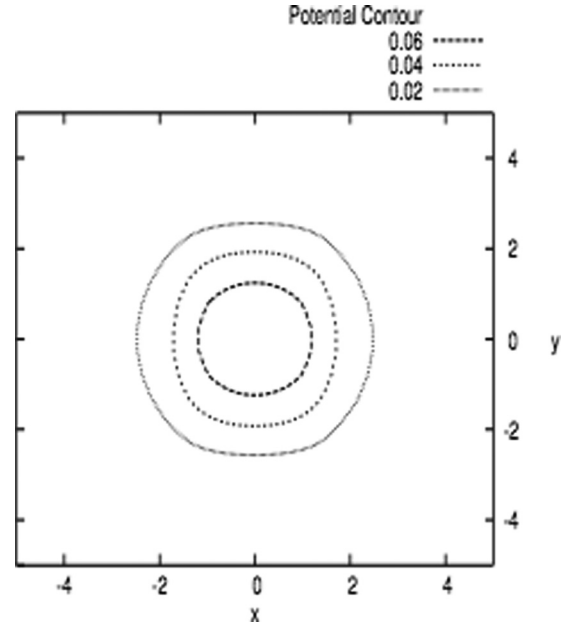
FIG. 5. Potential contour without flow feedback. Here, length are normalized in ρ_s. The other parameters used are $|f_H\Delta v_\parallel| = 0.1$, $\Delta x/\rho_s = \Delta y/\rho_s = 3.0$, $\rho_s/L_y = 0.03$, $\rho_* = 0.01$. The screening is symmetric and $E\times B$ vortex is symmetric.

detail below, the second term describes the shift of the $E\times B$ vortex while the third term describes the flow-hole resonance which enables energy transfer between drift hole and shear flow. Technically, these terms are expressed in terms of the integration involving the solution ϕ. To proceed, we approximate the ϕ in the integrand by $\phi^{(0)}$. This is analogous to the Born approximation in quantum mechanical particle scattering, where the actual scattered wave function is replaced by the zeroth order plane wave solutions.[27] Further, for simplicity we assume $\langle v_y\rangle \cong Sx$ in the following. The approximation of the flow structure simplifies the analysis by allowing the spatial integral to be performed straightforwardly, while we note that as a caveat, the flow profile should be in principle determined from coupled evolution of the drift hole and zonal flow.

The second term in Eq. (16) describes the deformation and shift of the $E\times B$ vortex. Using the approximation discussed above, the second term in Eq. (16) can be integrated to give

$$\frac{e\phi_k^{shift}}{T_e} = \frac{|f_H\Delta v_\parallel|}{2\chi^{3/2}}\left(\frac{k_yc_s}{k_\parallel u_\parallel}\right)^2\frac{S}{\omega_{ci}}\rho_*\frac{\Delta y}{L_y}\frac{2}{k_y\Delta y}$$
$$\times\sin\left(\frac{k_y\Delta y}{2}\right)X_k^{shift}(x), \quad (21)$$

where $X_k^{shift}(x)$ is a function which determines the radial structure of ϕ_k^{shift}. $X_k^{shift}(x)$ is defined as

$$X_k^{shift}(x) \equiv \left[I_{in} - \frac{1}{2}\left(\frac{\Delta x^2}{4\rho_s^2} - \frac{x^2}{\rho_s^2}\right)\exp\left(-\frac{\Delta x}{2\lambda_k}\right)\right]$$
$$\times\sinh\frac{x}{\lambda_k} + \frac{2x}{\chi\lambda_k} - \frac{x}{2\rho_s\sqrt{\chi}}\exp\left(-\frac{\Delta x}{2\lambda_k}\right)\cosh\frac{x}{\lambda_k},$$
$$(22)$$

for $|x| < \Delta x/2$ and

$$X_k^{shift}(x) \equiv \frac{x}{|x|}\exp\left(-\frac{|x|}{\lambda_k}\right)\left[I_{out} - \frac{1}{2}\left(\frac{\Delta x^2}{4\rho_s^2} - \frac{x^2}{\rho_s^2}\right)\right]$$

$$\times \sinh\frac{\Delta x}{2\lambda_k} + \frac{|x|}{2\sqrt{\chi}\rho_s}\sinh\frac{\Delta x}{2\lambda_k}\bigg], \tag{23}$$

for $|x| > \Delta x/2$. The constants I_{in} and I_{out} are defined as

$$I_{in} \equiv \frac{1}{2\chi}\left(1 + \frac{\Delta x}{\lambda_k}\right)\exp\left(-\frac{\Delta x}{\lambda_k}\right) - \frac{1}{\chi}\left(\frac{7}{4} + \frac{\Delta x}{\lambda_k}\right)\exp\left(-\frac{\Delta x}{2\lambda_k}\right)$$
$$+ \frac{1}{4\chi}\left(1 + \frac{\Delta x}{\lambda_k}\right)\exp\left(-\frac{3\Delta x}{2\lambda_k}\right) \tag{24}$$

and

$$I_{out} \equiv -\frac{1}{4\chi}\left[7 + \left(1 + \frac{\Delta x}{\lambda_k}\right)\exp\left(-\frac{\Delta x}{\lambda_k}\right)\right]\sinh\frac{\Delta x}{2\lambda_k}$$
$$+ \frac{1}{4\chi}\exp\left(-\frac{\Delta x}{2\lambda_k}\right)\sinh\frac{\Delta x}{\lambda_k}$$
$$+ \frac{\Delta x}{\chi\lambda_k}\left(\cosh\frac{\Delta x}{2\lambda_k} - \frac{1}{4}\exp\left(-\frac{\Delta x}{2\lambda_k}\right)\cosh\frac{\Delta x}{\lambda_k}\right). \tag{25}$$

To see the effect of ϕ^{shift}, we plot $\phi = \sum_{k_y}(\phi_k^{(0)} + \phi_k^{shift})$ $\exp(ik_yy)$ in Fig. 6. As compared to $\phi^{(0)}$ (Fig. 5), the potential is clearly deformed by the shear flow. In particular, the potential lacks reflectional symmetry in x, and is shifted radially. This is because the shear flow introduces a spatial dependence to the screening length $\lambda[\langle v_y(x)\rangle]$. The spatial dependence leads to different screening responses for $x > 0$ and $x < 0$, which leads to the overall radial shift of the $E \times B$ vortex. We note that the analysis and the result given here are analogous to the well-known shear flow effect[19] on the eigen-

Potential Contour
0.06 ·······
0.04 ········
0.02 ------
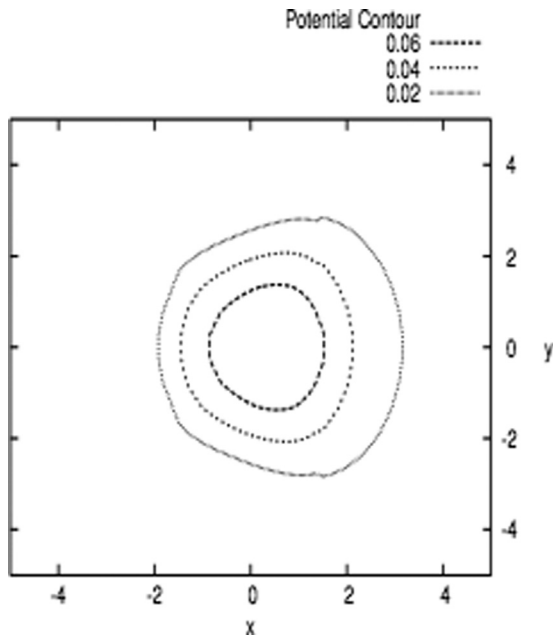
FIG. 6. Potential contour with flow feedback ($\langle v_y\rangle = Sx$, external flow). Here, length are normalized in ρ_s. The other parameters used are $|f_H\Delta v_\parallel| = 0.1$, $\Delta x/\rho_s = \Delta y/\rho_s = 3.0$, $\rho_s/L_y = 0.03$, $\rho_* = 0.01$, $\rho_*\omega_{ci}/(k_\parallel u_\parallel) = 1.0$, $S/\omega_{ci} = 0.05$. The potential is screened more strongly for $x < 0$ than for $x > 0$, resulting in a shifted, deformed $E \times B$ vortex.

mode structure of drift waves,[20] where a shear flow breaks the eigenfunction symmetry around the rational surface and shifts the eigenmode potential radially.

The third term in Eq. (16) is related to flow-hole resonance. The integration can be performed to give

$$\frac{|e|\phi_k^{res}}{T_e} = \frac{i\pi}{2\sqrt{\chi}}\exp\left(-\frac{|x - x_c|}{\lambda_k}\right)\frac{c_s}{|S||L_n|}\frac{k_y}{|k_y|}\frac{|e|\phi_k^{(0)}(x_c)}{T_e}, \tag{26}$$

where x_c is the location of the hole-flow resonance (i.e., the location of the critical layer), i.e.,

$$x_c = \frac{k_\parallel}{k_y}\frac{u_\parallel}{S}. \tag{27}$$

This term physically describes the coupling of the drift hole structure to the plasma flow via a dissipative resonance. The localized structure produces a screening field, as depicted in Fig. 7. The resonance allows the energy in the screening field to be radiated and absorbed into the flow. As a result, the localized structure feels the presence of the flow through the screening field, whose effect appears as ϕ^{res}. Stated differently, the structure and the flow form a single entity through the absorption process.

An important feature of the resonance process is that it enables the coupling between drift holes and zonal flows by allowing the necessary finite cross phase in the Reynolds stress, to produce a momentum flux. The momentum is ($\langle ...\rangle$ denotes average in y and z direction)

$$\langle\tilde{v}_x\tilde{v}_y\rangle = \frac{c^2}{B^2}\text{Re}\sum_k ik_y(\phi_{-k}^{(0)} + \phi_{-k}^{shift} + \phi_{-k}^{res})$$
$$\times \partial_x(\phi_k^{(0)} + \phi_k^{shift} + \phi_k^{res}). \tag{28}$$

Noting $\phi_k^{(0)}$ and ϕ_k^{shift} are purely real and ϕ_k^{res} is purely imaginary, the non-zero contribution comes from the terms involving ϕ_k^{res} as

$$\langle\tilde{v}_x\tilde{v}_y\rangle = \frac{c^2}{B^2}\text{Re}\sum_k ik_y(\phi_{-k}^{(0)} + \phi_{-k}^{shift})\partial_x\phi_k^{res}$$
$$+ \frac{c^2}{B^2}\text{Re}\sum_k ik_y\phi_{-k}^{res}\partial_x(\phi_k^{(0)} + \phi_k^{shift}). \tag{29}$$

Structure
+ Screening Potential

Absorption Points
$\rightarrow$ Zonal Flow Coupling
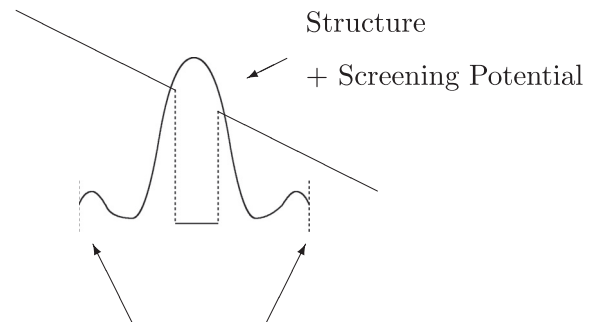
FIG. 7. Drift hole and zonal flow coupling.

The fact that the drift hole is coupled to zonal flows requires us to incorporate zonal flows into the dynamics of the drift hole as well. The dynamical dependence of drift hole growth on zonal flows is discussed in Sec. III.

To summarize, the total potential was obtained as

$$\frac{|e|\phi_k}{T_e} = \frac{|e|\phi_k^{(0)}}{T_e} + \frac{|e|\phi_k^{shift}}{T_e} + \frac{|e|\phi_k^{res}}{T_e}. \quad (30)$$

$\phi^{(0)}$ describes the isotropic $E \times B$ vortex, Fig. 5. ϕ^{shift} and ϕ^{res} arise due to flow, which influences drift hole potential structure by changing the plasma medium response and thus the screening effect. ϕ^{shift} gave a shift to the isotropic $E \times B$ vortex (Fig. 6), which is similar to the shift of drift wave eigenmode structure. ϕ^{res} is related to the flow-hole resonance, which allows the zonal flow to absorb energy or momentum of the screening field.

III. DRIFT HOLE DYNAMICS AND TURBULENCE DRIVEN FLOWS

Once formed, drift hole structure can grow by extracting free energy. Simply put, the growth is caused by a hole being displaced up the background gradient, as depicted in Fig. 8. As a hole is displaced up the gradient, since f_e is conserved, its depth $\delta f_e = f_e - \langle f_e \rangle$ must grow.[4,6,11] For an electron drift hole, the displacement is made possible by scattering off ions. The scattering of ions requires the electron structure to move up the gradient so as to maintain the quasi-neutrality constraint. This enables the electron hole to be displaced in phase space and to grow.

A. Drift hole growth with turbulence driven flows

To describe the growth of a drift hole, we consider a displacement of the drift hole in phase space from $(x_0, u_\parallel)$ to $(x, v_\parallel)$. Let phase space density at the initial position $\langle f_e \rangle|_0 + f_{H0}$ and at the displaced position $\langle f_e \rangle + f_H$ (Fig. 8). Since phase space density is conserved along trajectory, the two values must be same

$$\langle f_e \rangle|_0 + f_{H0} = \langle f_e \rangle + f_H. \quad (31)$$

From this, the increment in the depth of the hole $\delta f_e \equiv f_H - f_{H0}$ is calculated to be
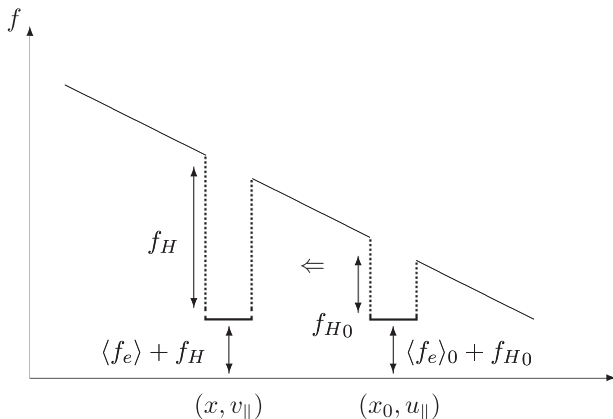
FIG. 8. Configuration of hole displacement.

$$\delta f_e = \langle f_e \rangle|_0 - \langle f_e \rangle \simeq -(x - x_0) \frac{\partial \langle f_e \rangle}{\partial x}\bigg|_0 - (v_\parallel - u_\parallel) \frac{\partial \langle f_e \rangle}{\partial v_\parallel}\bigg|_0. \quad (32)$$

The growth of the depth along the trajectory is then

$$\frac{d}{dt}\delta f_e^2 = 2\delta f_e \frac{d}{dt}\delta f_e \quad (33)$$

$$= 2\delta f_e \left(-\tilde{v}_x \frac{\partial \langle f_e \rangle}{\partial x}\bigg|_0 + \frac{|e|}{m_e}\tilde{E}_\parallel \frac{\partial \langle f_e \rangle}{\partial v_\parallel}\bigg|_0 \right), \quad (34)$$

where we used

$$\frac{d}{dt}(x - x_0) = \tilde{v}_x = \frac{c}{B}\tilde{E}_y, \quad \frac{d}{dt}(v_\parallel - u_\parallel) = -\frac{|e|}{m_e}\tilde{E}_\parallel. \quad (35)$$

Integrating over $v_\parallel$ and averaging over y and z, we obtain

$$\frac{\partial}{\partial t}\int dv_\parallel \frac{\langle \delta f_e^2 \rangle}{2} = -\left\langle \tilde{v}_x \frac{\delta n_e}{n_0} \right\rangle \frac{\partial \langle f_e \rangle}{\partial x}\bigg|_0 + \frac{|e|}{m_e}\left\langle \tilde{E}_\parallel \frac{\delta n_e}{n_0} \right\rangle \frac{\partial \langle f_e \rangle}{\partial v_\parallel}\bigg|_0. \quad (36)$$

Now, the electron drift hole growth is constrained by other charges via the quasi-neutrality condition. Since $\delta n_e = \delta n_i^{GC} + n_0\rho_s^2\nabla_\perp^2 e\phi/T_e$, the evolution of drift hole perturbation is given by

$$\frac{\partial}{\partial t}\int dv_\parallel \frac{\langle \delta f_e^2 \rangle}{2} = -\left\langle \tilde{v}_x \frac{\delta n_i^{GC}}{n_0} \right\rangle \frac{\partial \langle f_e \rangle}{\partial x}\bigg|_0$$
$$+ \frac{|e|}{m_e}\left\langle \tilde{E}_\parallel \frac{\delta n_i^{GC}}{n_0} \right\rangle \frac{\partial \langle f_e \rangle}{\partial v_\parallel}\bigg|_0$$
$$- \left\langle \tilde{v}_x \rho_s^2\nabla_\perp^2 \frac{e\tilde{\phi}}{T_e} \right\rangle \frac{\partial \langle f_e \rangle}{\partial x}\bigg|_0$$
$$+ \frac{|e|}{m_e}\left\langle \tilde{E}_\parallel \rho_s^2\nabla_\perp^2 \frac{e\tilde{\phi}}{T_e} \right\rangle \frac{\partial \langle f_e \rangle}{\partial v_\parallel}\bigg|_0. \quad (37)$$

Thus, the overall growth is determined by the spatial and velocity scattering of guiding center ion and polarization charge. Simply put, to climb up the gradient, electron drift hole must scatter guiding center ion and polarization charge to satisfy quasi-neutrality.

The first two terms due to the guiding center ions are the drive of drift hole instability, as discussed in an earlier study. Writing $\delta n_i^{GC}/n_0 = \chi_i(e\phi/T_e)$, we have

$$-\left\langle \tilde{v}_x \frac{\delta n_i^{GC}}{n_0} \right\rangle \frac{\partial \langle f_e \rangle}{\partial x}\bigg|_0 + \frac{|e|}{m_e}\left\langle \tilde{E}_\parallel \frac{\delta n_i^{GC}}{n_0} \right\rangle \frac{\partial \langle f_e \rangle}{\partial v_\parallel}\bigg|_0$$
$$= -\langle f_e \rangle|_0 \sum_{\mathbf{k}}(\omega_{*e}|_0 - k_\parallel u_\parallel)\text{Im}\chi_i(\mathbf{k}, k_\parallel u_\parallel)\left| \frac{e\tilde{\phi}}{T_e} \right|_{\mathbf{k}}^2. \quad (38)$$

Here, $\omega_{*e}|_0 = -k_y\rho_s c_s\partial_x\ln\langle f_e \rangle|_0 \simeq \omega_{*e}(1 - \eta_e/2)$ ($u_\parallel < v_{the}$ was assumed), the frequency ω is evaluated at hole Doppler frequency $\omega = k_\parallel u_\parallel$, $\mathbf{k}$ refers to modes excited by the drift hole, and $\text{Im}\chi_i$ is the imaginary part of the guiding center ion susceptibility. Note that here ion dissipation $\text{Im}\chi_i$ acts as a trigger of instability. This is quite different from the usual drift wave instability, where ion dissipation is a stabilizing effect. The dissipation $\text{Im}\chi_i$ is a necessary ingredient for drift

hole instability, since such instability requires the irreversible scattering of guiding center ions via the quasi-neutrality constraint.

The third and the fourth terms in Eq. (37) are associated with polarization charge. Physically, these terms are related to zonal and toroidal flows. The connection may be best seen by noting the identities

$$\langle \tilde{v}_x \nabla_\perp^2 \tilde{\phi} \rangle = -\frac{c}{B}\partial_x \langle \partial_y \tilde{\phi} \partial_x \tilde{\phi} \rangle = \frac{B}{c}\partial_x \langle \tilde{v}_x \tilde{v}_y \rangle \quad (39)$$

and

$$\langle \tilde{E}_\parallel \nabla_\perp^2 \tilde{\phi} \rangle = -\partial_x \langle \partial_z \tilde{\phi} \partial_x \tilde{\phi} \rangle + \frac{1}{2}\partial_z \langle (\partial_x \tilde{\phi})^2 \rangle$$
$$- \partial_y \langle \partial_z \tilde{\phi} \partial_y \tilde{\phi} \rangle + \frac{1}{2}\partial_z \langle (\partial_y \tilde{\phi})^2 \rangle$$
$$= -\partial_x \langle \tilde{E}_x \tilde{E}_\parallel \rangle. \quad (40)$$

The first identity relates polarization charge flux (vorticity flux) to the Reynolds force on zonal flow,[13,14] while the second one is related to the parallel acceleration of toroidal flow due to charge separation.[28,29] Thus, the drift hole instability is coupled to the generation of both zonal and toroidal flows. Of course, a finite cross-phase is required for non-zero contribution. The cross-phase of polarization charge scattering is set by flow-hole resonance, as follows. The spatial flux of polarization charge is written using the potential structure derived above as

$$\langle \tilde{v}_x \nabla_\perp^2 \tilde{\phi} \rangle = \frac{c}{B}\mathrm{Re}\sum_k ik_y(\phi_{-k}^{(0)} + \phi_{-k}^{shift} + \phi_{-k}^{res})$$
$$\times \partial_x^2(\phi_k^{(0)} + \phi_k^{shift} + \phi_k^{res}). \quad (41)$$

Due to its radial structure and phase, we have a non-zero contribution from the combination of ϕ^{shift} (pure real) and ϕ^{res} (pure imaginary) as

$$\langle \tilde{v}_x \nabla_\perp^2 \tilde{\phi} \rangle = \frac{c}{B}\mathrm{Re}\sum_k ik_y(\phi_{-k}^{shift}\partial_x^2\phi_k^{res} + \phi_{-k}^{res}\partial_x^2\phi_k^{shift}), \quad (42)$$

which leads to non-zero Reynolds forcing. Thus, the proper phase for polarization charge flux and thus Reynolds forcing is provided by the flow-hole resonance. A similar argument applies to the velocity scattering of polarization charge.

Having discussed each term in Eq. (37), we now discuss the implication for drift hole growth. Collecting the result, Eq. (37) now becomes

$$\frac{\partial}{\partial t}\int dv_\parallel \frac{\langle \delta f_e^2 \rangle}{2} = -\langle f_e \rangle|_0 \sum_{\mathbf{k}}(\omega_{*e}|_0 - k_\parallel u_\parallel)\mathrm{Im}\chi_i \left|\frac{e\tilde{\phi}}{T_e}\right|_{\mathbf{k}}^2$$
$$- \frac{1}{\omega_{ci}}\partial_x \langle \tilde{v}_x \tilde{v}_y \rangle \frac{\partial \langle f_e \rangle}{\partial x}\bigg|_0$$
$$- \frac{m_i}{m_e}\frac{c^2}{B^2}\partial_x \langle \tilde{E}_x \tilde{E}_\parallel \rangle \frac{\partial \langle f_e \rangle}{\partial v_\parallel}\bigg|_0. \quad (43)$$

The first term is due to the scattering of guiding center ions, while the second and the third terms are due to the scattering of polarization charge. Here, we first consider a "bare"

growth, i.e., without flow coupling, and later come back to the issue of flows. For the growth rate, we derive its scaling property. Using $|e\tilde{\phi}/T_e|_k^2 \sim \int dv_{\parallel,1}dv_{\parallel,2}\langle \delta f_e(1)\delta f_e(2)\rangle_k/|\chi|^2$ via the GK Poisson equation, $\int dv_\parallel \delta f_e \sim \Delta v_\parallel \delta f_e$, and $\mathrm{Im}\chi_i < 0$ for ion Landau damping, we have

$$\gamma \Delta v_\parallel \langle \delta f_e^2 \rangle \sim \langle f_e \rangle|_0 (\omega_{*e}|_0 - k_\parallel u_\parallel)(|\mathrm{Im}\chi_i|)\frac{\Delta v_\parallel^2 \langle \delta f_e^2 \rangle}{|\chi|^2}. \quad (44)$$

This estimate then yields a scaling form of the growth rate as

$$\gamma \sim \langle f_e \rangle|_0 \Delta v_\parallel(\omega_{*e}|_0 - k_\parallel u_\parallel)\frac{|\mathrm{Im}\chi_i|}{|\chi|^2} \sim k_\parallel \Delta v_\parallel \frac{|\mathrm{Im}\chi_e \mathrm{Im}\chi_i|}{|\chi|^2}. \quad (45)$$

We can extract several features of drift hole instability from Eq. (45). First of all, the growth rate is nonlinear, as it depends on amplitude via $\Delta v_\parallel \sim \sqrt{\tilde{\phi}}$. This allows explosive, rather than linear exponential growth, of fluctuations. Second, the instability requires a free energy, $\gamma \propto \omega_{*e}|_0 - k_\parallel u_\parallel$. The requirement that $\omega_{*e}|_0 - k_\parallel u_\parallel > 0$ for instability means that spatial scattering has to release more energy than the cost due to velocity scattering, similar to $\omega < \omega_{*e}$ for drift wave instability. Finally, the drift hole instability is triggered by ion dissipation $\mathrm{Im}\chi_i$. Ion dissipation is essential for drift hole instability since it allows irreversible scattering of ions and thus non-zero ion flux. Due to the quasi-neutrallity condition, the non-zero ion flux allows an electron hole to be displaced up the gradient, and thereby to access free energy, as depicted in Fig. 8.

The feature of the drift hole instability can be further clarified by comparing it to the linear growth of drift waves, Table I. Both instabilities require free energy to grow, i.e., $\omega_{*e}|_0 > k_\parallel u_\parallel$ for the drift hole instability and $\omega_{*e} > \omega$ for the linear drift wave instability. On the other hand, the drift hole instability is distinctive in that it is nonlinear and triggered by ion dissipation. The drift hole instability is amplitude dependent $\gamma \sim \Delta v_\parallel$ and thus allows nonlinear explosive growth, while the electron drift wave instability is independent of amplitude and thus gives exponential linear growth. In addition, the drift hole instability is triggered by $\mathrm{Im}\chi_i$, while the linear instability is damped by $\mathrm{Im}\chi_i$. Due to the different dependence on $\mathrm{Im}\chi_i$, we note that the growth of the hole can be subcritical, i.e., $\gamma > 0$ even when $\gamma_L \lesssim 0$. This allows release of free energy even when plasmas are linearly stable or only weakly unstable, and thus drift hole structures can be more efficient at tapping free energy than drift wave eigenmodes.

We also note that a similar scaling form as Eq. (45) is obtained for a subcritical hole instability in 1D Vlasov system with a bump on tail and a generic background dissipation.[5] The result for the 1D Vlasov system qualitatively agrees with a simulation result.[9] Table II shows a comparison between the results from the GK calculation and the 1D Vlasov calculation.

The drift hole instability is coupled to zonal and toroidal flows, as explicitly seen in Eq. (43). This leaves a footprint on the drift hole growth. Namely, by scattering polarization

TABLE I. Comparison between linear and nonlinear instabilities.

	Electron drift wave instability	Electron drift hole instability
Growth rate	$\gamma_L \sim \|\partial\chi/\partial\omega_k\|^{-1}(\|\mathrm{Im}\chi_e\| - \|\mathrm{Im}\chi_i\|)$	$\gamma \sim k_\|\Delta v_\| \|\mathrm{Im}\chi_e \mathrm{Im}\chi_i\|/\|\chi\|^2$
Access to free energy	$\omega_* > \omega$	$\omega_{*e}\|_0 > k_\| u_\|$
Amplitude dependence	No	Yes, $\propto \Delta v_\| \sim \sqrt{\tilde\phi}$
Ion Landau damping	Stabilizing	Destabilizing
Type of instability	Supercritical, exponential growth	Subcritical, explosive growth

charges, the drift hole is coupled to zonal flows (and toroidal flows). The coupling is made possible via hole-flow resonance, which provides the proper phase for polarization scattering. The flow coupling makes structure-induced mixing more difficult, resulting in the reduction of instability drive. The effect explicitly appears in Eq. (43), from which we can see that the dissipation driven via ion Landau damping must overcome the energy penalty due to the flow coupling.

Eventually, the flow coupling can saturate drift hole instability. Namely, while drift hole grows by extracting free energy, the growing hole keeps pumping turbulence driven flows via absorption arising from hole-flow resonance. The pumping amplifies the hole-flow resonance, and eventually makes the polarization scattering comparable to the guiding center ion scattering. This leads to the saturation of drift hole growth. In the following, we discuss a more precise treatment of the coupled dynamics of the drift hole-zonal flow system and its implication for the saturation of the drift hole growth.

B. Saturation of drift hole growth with turbulent driven flows and an upper bound on fluctuation amplitude

Here, we discuss the saturation of the nonlinear instability. Since the quasi-neutrality constraint on drift hole growth requires the scattering of polarization charge, drift hole turbulence is dynamically coupled to turbulence driven flows. Thus, the saturation of drift hole instability is a highly nonlinear phenomena involving the interplay between dynamically evolving turbulent fluctuations and turbulence driven flows. Explicitly, as seen in Eq. (43), the evolution of drift hole turbulence contains both the Reynolds force on the zonal flow and the polarization force on the toroidal flow. To describe the fully nonlinear dynamics of the coupled system, we need an evolution equation for the flows. For the zonal flow momentum balance, we employ a simplified model

$$\partial_t \langle v_y \rangle = -\partial_x \langle \tilde v_x \tilde v_y \rangle - \nu_d^\perp \langle v_y \rangle. \tag{46}$$

Here, the drive is given by the Reynolds force, and the damping is accounted for by $\nu_d^\perp$. For the toroidal flow, we note that forcing arises from *both* the momentum flux and the polarization forcing.[28,29] Since the toroidal flow coupling in Eq. (43) describes a part of the toroidal flow drive, fully coupled dynamics of the drift hole growth and toroidal flow generation requires modeling of the momentum flux (including residual stress) driven by the drift hole potential. However, this is beyond the scope of the paper and hereafter we focus on the zonal flow coupling in drift hole dynamics. Note that neglecting the toroidal flow feedback is consistent with restricting the analysis to $\omega_*\|_0 > k_\| u_\|$, since the ratio of zonal flow feedback to toroidal flow feedback in $\langle \delta f_e^2 \rangle$ evolution is

$$\left| -\frac{1}{\omega_{ci}}\partial_x \langle \tilde v_x \tilde v_y \rangle \frac{\partial \langle f_e \rangle}{\partial x}\Big|_0 \right| : \left| -\frac{m_i}{m_e}\frac{c^2}{B^2}\partial_x \langle \tilde E_x \tilde E_\| \rangle \frac{\partial \langle f_e \rangle}{\partial v_\|}\Big|_0 \right|$$
$$\sim |\omega_*| : |k_\| u_\||. \tag{47}$$

Eliminating the Reynolds force, we obtain the coupled evolution equation for drift hole turbulence and turbulence driven zonal flows

$$\frac{\partial}{\partial t}\left(\int dv_\| \frac{\omega_{ci}\langle \delta f_e^2 \rangle}{2\partial\langle f_e \rangle/\partial x\|_0} - \langle v_y \rangle \right) = \frac{c_s^2}{v_*}\sum_{\mathbf{k}}(\omega_{*e}\|_0 - k_\| u_\|)$$
$$\times \mathrm{Im}\chi_i \left| \frac{e\tilde\phi}{T_e} \right|_{\mathbf{k}}^2 + \nu_d^\perp \langle v_y \rangle, \tag{48}$$

where $v_* = (\rho_s/|L_n|)c_s(1 - \eta_e(1 - u_\|^2/v_{the}^2)/2)$. In the presence of flows, the growth of the structure must accompany the acceleration of zonal flow, as depicted in Fig. 2. The coupled evolution of the drift hole and zonal flow is analogous to the coupled evolution of turbulence and flows in a potential vorticity conserving, quasi-geostrophic system. For example, in the Hasewaga-Wakatani system[17] the coupled evolution is described by a momentum theorem[14]

TABLE II. Growth in 1D Vlasov vs. Gyrokinetic plasma. For 1D Vlasov plasma, "BOT" is "bump-on-tail," γ_d is a generic background dissipation, u is a resonant velocity, and ω_p is the plasma frequency.

	1D Vlasov plasma	Gyrokinetic plasma
Linear growth rate γ_L	$\gamma_{BOT} - \gamma_d$	$\|\partial\chi/\partial\omega_k\|(\|\mathrm{Im}\chi_e\| - \|\mathrm{Im}\chi_i\|)$
Nonlinear growth rate γ_{NL}	$\Delta v(\partial f_0/\partial v)\|_u u\gamma_d(\omega_p^2/(k^2 u^2 + 4\gamma_d^2))$	$f_e^{(0)}\Delta v_\|(\omega_{*e}\|_0 - k_\| u_\|)\|\mathrm{Im}\chi_i\|/\|\chi\|^2$
Dissipation	γ_d	$\mathrm{Im}\chi_i$
Subcritical growth	Yes	Yes

$$\frac{\partial}{\partial t}\left\{\frac{\langle\delta q^2\rangle}{2\langle q\rangle'}+\langle v_\theta\rangle\right\}=-\langle\tilde{v}_r\tilde{n}_e\rangle-\frac{1}{\langle q\rangle'}$$
$$\times\left(\frac{\partial}{\partial r}\langle\tilde{v}_r\frac{\delta q^2}{2}\rangle+D_0\langle(\nabla\delta q)^2\rangle\right)$$
$$-\nu\langle v_\theta\rangle. \qquad (49)$$

Here $q=n-\rho_s^2\nabla_\perp^2(e\phi/T_e)$, $\langle\delta q^2\rangle/\langle q\rangle'$ is the wave activity density, D_0 is the diffusivity of potential vorticity, and ν is a collisional drag on the flow. Here for simplicity the particle diffusivity (D_0) and the viscosity (μ) were assumed to be equal. The wave activity density is related to fluctuation pseudomomentum,[30] since in weak turbulence limit $\langle\delta q^2\rangle/\langle q\rangle'\sim-|v_*|^{-1}\sum_k(1+\rho_s^2k_\perp^2)^2|\hat{\phi}|_k^2\sim-\sum_k k_\theta(\mathcal{E}_k/\omega_k)$ which is recognizable as the negative of the wave momentum density. The theorem relates the coupled evolution of zonal flow momentum and fluctuation psedomomentum to the driving flux of turbulence, the local collisional dissipation of turbulence, turbulence spreading (the triplet term), and drag on zonal flow. Note that the turbulence spreading term can act as an effective local drive or dissipation of turbulence, depending on whether there is a local convergence or divergence of the potential enstrophy flux. The correspondence between the theorem and Eq. (48) is apparent. Here, Eq. (48) describes the coupled evolution of zonal flow momentum and the pseudomomentum of the drift hole. The drift hole pseudomomentum is given by $\langle\delta f_e^2\rangle/\langle f_e\rangle'$, which can be viewed as a kinetic extension of the wave activity density. It may be interesting to note that the kinetic pseudomomentum is related to several other quantities such as the phasetrophy[31,32] $\langle\delta f_e^2\rangle$ (potential enstrophy in phase space), fluctuation entropy $\int dv_\parallel\langle\delta f_e^2\rangle/\langle f_e\rangle$, as well as the fluctuation dynamic pressure $\int dv_\parallel\langle\delta f_e^2\rangle/(2\partial\langle f_e\rangle/\partial E|_0)$, defined in the context of the kinetic energy principle for the Jean's instability for self-gravitating matter.[33]

At this point, it may be appropriate to clarify the flow of free energy in the coupled dynamics of drift hole structure and zonal flow. The free energy channel is depicted in Fig. 9. Note Fig. 9 is specifically to an electron drift hole. The electron drift hole extracts free energy from the mean distribution function $\langle f_e\rangle$ by scattering guiding center ions and polarization charges. Scattering of guiding center ions leads to the growth of the drift hole structure, and hence releases the free energy. On the other hand, the quasi-neutrality constraint requires the structure to scatter polarization charge as well. This allows a part of the free energy to be coupled to zonal flows. Note zonal flows are a "benign" repository of the free energy, since they cannot cause any transport. Note
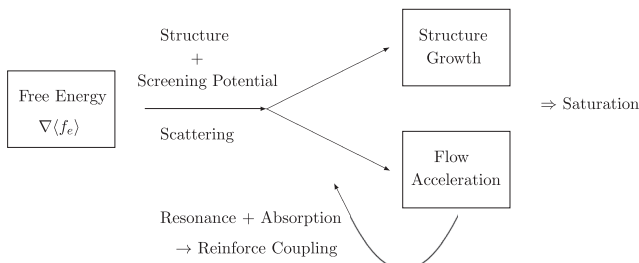
FIG. 9. Flow of free energy.

also that once accelerated, zonal flows reinforce the free energy coupling to the zonal flow channel. This is because the accelerated zonal flows can enhance the resonant absorption of drift holes. Zonal flow shears shift phases in the polarization charge flux further, and hence promote free energy coupling to the zonal flow channel.

The partition of the free energy leads to a self-regulating, predator-prey behavior of the drift hole and zonal flow. Here the prey is the drift hole, while the predator is the zonal flow. To address the point, it is useful to recall the predator-prey behavior of the *drift wave* and zonal flow system. A simplified model of drift wave and zonal flow turbulence is given as:

$$\partial_t\mathcal{E}_{DW}=\gamma_L\mathcal{E}_{DW}-\alpha\mathcal{E}_{DW}V_{ZF}'^2-\Delta\omega(\mathcal{E}_{DW})\mathcal{E}_{DW}, \qquad (50a)$$

$$\partial_t V_{ZF}'^2=\alpha\mathcal{E}_{DW}V_{ZF}'^2-\nu V_{ZF}'^2. \qquad (50b)$$

Here, $\mathcal{E}_{DW}$ is the energy of the drift wave, $V_{ZF}'^2$ is the energy of the zonal flow, γ_L is a linear growth rate of the drift wave, α is a coupling constant, $\Delta\omega$ is a nonlinear damping of the drift wave, and ν is a collisional damping of the zonal flow. The drift wave behaves as a prey, while the zonal flow behaves as a predator. The prey is excited by the linear growth. The damping of the prey is two fold; dissipation by itself and dissipation by coupling to the predator. The predator is supported by the prey, while the predator reduces its population by collisional damping. Through the coupling process, the total energy between the prey and the predator is conserved. The conservation is explicitly manifested by adding the coupled equations

$$\partial_t(\mathcal{E}_{DW}+V_{ZF}'^2)=\gamma_{eff}\mathcal{E}_{DW}-\nu V_{ZF}'^2. \qquad (51)$$

Here, $\gamma_{eff}\equiv\gamma_L-\Delta\omega(\mathcal{E}_{DW})$ is the difference between the linear growth rate and the nonlinear damping of the drift waves. Note that similar conservation relation holds for the coupled drift hole and zonal flow system (Eq. (48)), albeit Eq. (48) describes the momentum budget.

The coupling between drift hole and zonal flow can impact the saturation of drift hole growth. Due to the coupling, a stationary state is achieved with a non-zero zonal flow. The stationary state is achieved when the competing effects on the righthand side of Eq. (48) balance, i.e.,

$$0=\frac{c_s^2}{v_*}\sum_k(\omega_{*e}|_0-k_\parallel u_\parallel)\mathrm{Im}\chi_i\left|\frac{e\tilde{\phi}}{T_e}\right|_k^2+\nu_d^\perp\langle v_y\rangle.$$

We note that in principle, $\mathrm{Im}\chi_i$ can be a function of flows. Such flow dependence may allow a bifurcated flow solution. However, a detailed analysis of the bifurcated flow solution is beyond the scope of the paper and will be pursued in a future publication. Here, for simplicity, we assume $\mathrm{Im}\chi_i$ is set by ion Landau damping and is independent of the flow velocity. Given the caveat, stationary solution for the zonal flow is given by

$$\frac{\langle v_y\rangle}{c_s}=-\frac{1}{\nu_d^\perp}\frac{c_s}{v_*}\sum_k(\omega_{*e}|_0-k_\parallel u_\parallel)\mathrm{Im}\chi_i\left|\frac{e\tilde{\phi}}{T_e}\right|_k^2. \qquad (52)$$

Several remarks on the saturation and the resultant zonal flows are in order. First, the physical picture of saturation is that drift hole growth saturates when the mixing of phase space density with ion dissipation is suppressed by large enough dynamical friction from flows. This follows from the fact that since the total momentum is conserved, flows are accelerated from drift hole turbulence. Second, all that is required for flow generation is a drift hole—a localized single phase space structure—and the absorption of its momentum by the flow at the resonance. This is sharp contrast to the familiar concepts for zonal flow generation by turbulence, such as inverse cascade,[22] Rhine's scale,[23] modulational instability,[12] etc. This suggests that while the above mentioned familiar concepts are useful to understand zonal flow physics, none of them are fundamental. Finally, since drift holes and zonal flows form a self-regulating predator-prey system, the saturated state discussed here with non-zero zonal flow can be viewed as the stationary state of predator-prey system with a non-zero predator population.

We can extract the maximal saturation amplitude for drift hole-zonal flow turbulence from the saturated zonal flow velocity Eq. (52). The amplitude is obtained as follows. Namely, at saturated state, non-zero flows are required, while the resultant zonal flow can feedback on drift hole structure through its screening length. If the flows were strong enough to make $\text{Re}\chi[\langle v_y\rangle] < 0$ or at least $\text{Re}\chi[\langle v_y\rangle] \to 0$, then the screening potential is not localized, and hence a self-bound drift hole does not form. Hence, to have a stationary state with non-zero flows, the resultant flow speed must not exceed the limit for the formation of the self-bound drift hole. The condition for drift hole to be self-bound is expressed in terms of the susceptibility as $\text{Re}\chi[\langle v_y\rangle] > 0$, which gives

$$\frac{\langle v_y\rangle}{c_s} < \min\left(\frac{u_\parallel}{c_s}\frac{k_\parallel}{k_y}\frac{\chi^{(0)}}{1+k_y^2\rho_s^2}\right). \quad (53)$$

Here the minimum value ensures $\lambda_k^{-2} \propto \text{Re}\chi[\langle v_y\rangle] > 0$ for each k. The condition Eq. (53) can be restated that hole-flow resonance is not strong, since the condition loosely says $k_y\langle v_y\rangle < k_\parallel u_\parallel$. This is physically plausible since if the resonance is strong, then the energy in the screening field is radiated and absorbed into the flows. In such cases, since the screening field is radiated away, the drift hole cannot self-bind itself.

The bounds on potential amplitude are then set by the condition Eq. (53), since the zonal flow is a function of fluctuation, i.e., $\langle v_y\rangle = \langle v_y\rangle[|\tilde\phi|^2]$ (see Eq. (52)). To be specific, we consider the saturation in the limit $\omega_{*e}|_0 \gg k_\parallel u_\parallel$, i.e., above threshold for drift hole growth. In this limit, the zonal flow level obtained from Eq. (48) is

$$\frac{\langle v_y\rangle}{c_s} \cong -\frac{\omega_{ci}}{\nu_d^\perp}\sum_{\mathbf{k}} k_y\rho_s\text{Im}\chi_i\left|\frac{e\tilde\phi}{T_e}\right|_{\mathbf{k}}^2. \quad (54)$$

Applying the condition $\langle v_y\rangle < \langle v_y\rangle_{max}$, the bound on potential amplitude in drift hole-zonal flow turbulence then is:

$$\left|\frac{e\tilde\phi}{T_e}\right|^2 < \left|\frac{e\tilde\phi}{T_e}\right|_{max}^2, \quad (55)$$

where the maximum amplitude is estimated to be

$$\left|\frac{e\tilde\phi}{T_e}\right|_{max}^2 \equiv \frac{\nu_d^\perp}{\omega_{ci}}\frac{1}{\rho_s k_y\text{Im}\chi_i}\min\left(\frac{u_\parallel}{c_s}\frac{k_\parallel}{k_y}\frac{\chi^{(0)}}{1+k_y^2\rho_s^2}\right). \quad (56)$$

Here $\overline{(\ldots)}$ denotes the spectral average. Note the zonal flow damping $\nu_d^\perp$ appears as a control parameter for the maximum amplitude. This is similar to the case in predator-prey models,[12,16] where the damping of the predator (zonal flow) controls the population of the prey (drift hole). Physically put, this is because a larger collisional damping damps the zonal flow more strongly. The strong damping of the zonal flow allows the drift hole to easily extract the free energy, which in turn leads to a larger fluctuation amplitude. As a caveat, however, we note that there are both an upper and lower limit on the collisional damping $\nu_d^\perp$. The upper bound[34] is necessary since if the collisional damping is too strong, then zonal flows are completely damped, and hence cannot act as a repository of free energy. On the other hand, the lower bound is tied to stability of the zonal flow. If the collisional damping is too weak, then the free energy coupling to zonal flow is so strong that the resultant zonal flow can become Kelvin-Helmholtz unstable.[35]

IV. CONCLUSION AND DISCUSSION

In this paper, we discussed the theory of drift hole structure and dynamics in the presence of zonal flows. In contrast to a previous study,[11] we emphasized, throughout, the role of self-consistent turbulence driven flows in determining the radial structure of drift hole potential and in describing nonlinear dynamics of drift hole growth. (See Table III for comparison to the previous study.) The principal results of the paper are:

1. The drift hole potential was determined as $\phi = \phi^{(0)} + \phi^{shift} + \phi^{res}$ by solving the Gyrokinetic Poisson equation with flow coupling. $\phi^{(0)}$ is the potential without flow coupling. This term describes an isotropic $E \times B$ vortex, as discussed in a previous study. In addition to $\phi^{(0)}$, here we have novel pieces due to flow coupling, i.e., ϕ^{shift} and ϕ^{res}. ϕ^{shift} originates from the expansion of the plasma susceptibility in terms of flow. Physically ϕ^{shift} describes radial shift of the isotropic $E \times B$ vortex, which is analogous to a

TABLE III. Comparison between a previous study (Terry, Diamond, and Hahm'90) and this work.

	Terry, Diamond, and Hahm'90	This work
Drift hole potential	$\phi^{(0)}$	$\phi^{(0)} + \phi^{shift} + \phi^{res}$
Time evolution	$\partial_t\int dv_\parallel\langle\delta f_e^2\rangle$	$\frac{\partial}{\partial t}\left(\int dv_\parallel\frac{\omega_{ci}\langle\delta f_e^2\rangle}{2\partial\langle f_e\rangle/\partial x|_0} - \langle v_y\rangle\right)$
Saturated amplitude	$\left|\frac{e\tilde\phi}{T_e}\right| \sim \frac{1}{\chi^{(0)}}\frac{\Delta x}{|L_n|}$	$\left|\frac{e\tilde\phi}{T_e}\right|_{max}^2 = \frac{\nu_d^\perp}{\omega_{ci}}\frac{1}{\rho_s k_y\text{Im}\chi_i}$ $\min\left(\frac{u_\parallel}{c_s}\frac{k_\parallel}{k_y}\frac{\chi^{(0)}}{1+k_y^2\rho_s^2}\right)$

flow shear effect on radial eigenmode structure of drift waves. ϕ^{res} originates from hole-flow resonance. This term gives rise to a cross-phase for Reynolds force, $\partial_x \langle \tilde{v}_x \tilde{v}_y \rangle$.

2. The theory of fully nonlinear dynamics of a drift hole and zonal flow was formulated. The dynamical evolution of the drift hole was coupled to the zonal flow, since the quasi-neutrallity constraint requires the drift hole to scatter polarization charge during hole growth. Since the polarization charge scattering is equivalent to Reynolds force on zonal flow, drift hole growth must be dynamically coupled to zonal flows. The coupled evolution of the drift hole and zonal flow is described by

$$\frac{\partial}{\partial t} \left(\int dv_\parallel \frac{\omega_{ci} \langle \delta f_e^2 \rangle}{2 \partial \langle f_e \rangle / \partial x |_0} - \langle v_y \rangle \right) = \frac{c_s^2}{v_*} \sum_{\mathbf{k}} (\omega_{*e}|_0 - k_\parallel u_\parallel)$$
$$\times \mathrm{Im}\chi_i \left| \frac{e\tilde{\phi}}{T_e} \right|^2_{\mathbf{k}} + \nu_d^\perp \langle v_y \rangle.$$

The coupled evolution describes a momentum budget of the drift hole and zonal flow. Due to the zonal flow coupling, it is the coupled momentum that evolves in time. Note this reduces to the expression for drift hole growth without flow coupling derived in an earlier study

$$\frac{\partial}{\partial t} \int dv_\parallel \frac{\langle \delta f_e^2 \rangle}{2} = -\langle f_e \rangle|_0 \sum_{\mathbf{k}} (\omega_{*e}|_0 - k_\parallel u_\parallel) \mathrm{Im}\chi_i \left| \frac{e\tilde{\phi}}{T_e} \right|^2_{\mathbf{k}}.$$

We note that the drift hole growth (up to flow) is subcritical, with the growth rate $\gamma_{NL} \sim k_\parallel \Delta v_\parallel |\mathrm{Im}\chi_i \mathrm{Im}\chi_e|/\chi^2$. This is quite different from the expression for the linear growth of drift waves, $\gamma_L \sim |\omega_*|(|\mathrm{Im}\chi_e| - |\mathrm{Im}\chi_i|)$.

3. The coupled evolution equation for the drift hole and zonal flow was analogous to momentum theorems which describe the coupled evolution of fluctuation pseudomomentum and flow momentum. $\int dv_\parallel \langle \delta f_e^2 \rangle / \langle f_e \rangle'$ is pseudomomentum of an electron drift hole, a kinetic expression similar to wave activity density for quasi-geostrophic turbulence. As a consequence of the coupling, it is not the drift hole pseudomomentum but the total momentum, including zonal flow momentum, that evolves in time. We argued that a stationary state is achieved when the total momentum is constant in time.

4. The coupled evolution equation for the drift hole and zonal flow was also interpreted in the context of a predator-prey system. Here, the drift hole is the prey, and the zonal flow is the predator. The self-regulating behavior was analogous to that for the drift wave-zonal flow system.

5. As a consequence of the coupled evolution, a stationary state is possible with flow coupling. At the stationary state, non-zero zonal flow is supported, and is given by

$$\frac{\langle v_y \rangle}{c_s} = -\frac{1}{\nu_d^\perp} \frac{c_s}{v_*} \sum_{\mathbf{k}} (\omega_{*e}|_0 - k_\parallel u_\parallel) \mathrm{Im}\chi_i \left| \frac{e\tilde{\phi}}{T_e} \right|^2_{\mathbf{k}}.$$

The saturated state is analogous to a state in the predator-prey system with non-zero predator population.

6. An upper bound on the drift hole potential amplitude in the coupled drift hole-zonal flow system was calculated.

The derivation was based on physical arguments that; (i) energy in the screening field of a drift hole is absorbed into flows and thus excites zonal flow, (ii) the coupling leads to a non-zero zonal flow at stationary state, and (iii) the resultant zonal flow velocity must not exceed the flow velocity above which a self-bound drift hope cannot form. The result predicts that

$$\left| \frac{e\tilde{\phi}}{T_e} \right|^2_{max} = \frac{\nu_d^\perp}{\omega_{ci}} \frac{1}{\rho_s k_y \mathrm{Im}\chi_i} \min \left(\frac{u_\parallel}{c_s} \frac{k_\parallel}{k_y} \frac{\chi^{(0)}}{1 + k_y^2 \rho_s^2} \right).$$

Note the appearance of the damping of zonal flow as a control parameter. The result can be compared to a saturation amplitude in a previous study[11] without flow coupling

$$\frac{\tilde{n}}{n_0} \sim \frac{\tilde{f}}{f_0} \sim \chi^{(0)} \left| \frac{e\tilde{\phi}}{T_e} \right| \sim \frac{\Delta x}{|L_n|}.$$

This is essentially the mixing length estimate. The result obtained here shows that the zonal flow enters saturation dynamics as a critical element. In particular, the zonal flow damping appears as a control parameter of the saturation amplitude.

Since the drift hole solution was obtained as a BGK solution for 3D magnetized plasmas, the drift hole can be viewed as analogous to a soliton. In this sense, the drift hole structure discussed here may be viewed as that analogous to a soliton solution in drift wave-zonal flow system,[36,37] which can spread turbulence. However, the drift hole solution obtained in this work is more general than the soliton solutions described in Refs. 36 and 37, since the drift hole solution includes resonant coupling with zonal flows. As shown above, such resonant coupling with zonal flows significantly influences the dynamical evolution of the drift hole soliton. This raises a question regarding the effect of the resonant coupling with zonal flows on drift wave-zonal flow solitons. The role of such dissipative resonant coupling of zonal flows in the soliton solutions in drift wave-zonal flow system will be pursued in a future publication.

While in this paper we are primarily concerned with *electron* drift holes, ion holes can be important in the theory of the relaxation by sub-marginal ITG turbulence. Here, we note that the relevance of such ion holes in sub-marginal ITG turbulence vary for different types of ITGs with different non-adiabatic electron response. This is because the non-adiabatic electron response can give rise to a non-zero electron particle flux. Such non-zero electron particle flux is required for ion holes to extract free energy while maintaining the quasi-neutrality. For example, for trapped ion resonance driven ITG turbulence with collisional non-adiabatic electron response, the electron particle flux is non-zero, hence ion holes *can* extract free energy. Indeed, the coupled evolution of ion holes and zonal flows in trapped ion driven ITG turbulence can be formulated as a momentum theorem, which is analogous to the momentum theorem (Eq. (48)) derived in the present paper for electron drift holes and zonal

flows. A detailed discussion of the coupled dynamics of ion holes and zonal flows for trapped ion driven ITG turbulence is found in Ref. 38. While for reactive ITG turbulence with adiabatic electron response, the electron particle flux is zero, thus, ion holes cannot extract free energy. In this case, dynamics of structure will be described by the conservation of ion pseudomomentum and zonal flow momentum (up to flow damping). More specifically, the conservation relation will be given by that analogous to Eq. (48) with the righthand side set to zero.

As a caveat, we note that the analysis presented here was concerned with a single coherent structure. Differently put, we considered *coherent* trapping. In contrast, as a complementary case, we can also have *turbulent* trapping, in which case structures form, but also break apart, leading to incoherent granular fluctuations.[38–42] While the analysis with the granulation requires a statistical treatment, rather than consideration of displacement of a single structure, the role of the granulation in driving relaxation is quite similar to the role of drift holes discussed here. Namely, the granulation evolves in time via dynamical friction due to the quasineutrality constraint, and can extract free energy even when plasmas are linearly stable. The granulation can also drive zonal flow by scattering polarization charge.

Taken together, we conclude that structures which form with either coherent or turbulent trapping are important players in relaxation in turbulent plasmas. Structures can directly extract free energy, which leads to profile relaxation. Structures (even a single structure) also can excite zonal flows, and possibly toroidal flows. These findings are in sharp contrast to profile relaxation and flow generation by quasi-linear drift wave turbulence, a paradigm which is often assumed in the fusion community.

The paradigm presented here may be applied to several issues in tokamak phenomenologies. As an example, we here discuss the application of this paradigm to the phenomenology of "No Man's Land." "No Man's Land" is a region that connects the tokamak core region to the tokamak edge-pedestal region (Fig. 10). An issue is that while the turbulence level is observed to increase from the core to the edge region, most theoretical predictions based on the local gradient driven instabilities cannot reproduce the observed turbulence profile. In particular, most theoretical predictions reproduce the core turbulence level, while the prediction of the turbulence level

FIG. 10. Incoming structures and turbulence in "No Man's Land."

deviates from the observed level in the connecting region. Here we argue that structures may enhance the turbulence level in the connecting region as follows. At the tokamak edge, a strong perturbation can nucleate structures such as density blobs or holes[1,2] (Fig. 10). Once formed, the blob propagates down the gradient, while the hole can propagate *up* the gradient. So, the hole can propagate *inward* from the edge and bombard the edge-core coupling region. As discussed above, since such incoming holes can tap free energy stored in the local gradient, such incoming holes can increase the turbulence level in the coupling region by feeding off the local gradient drive. Of course, the density holes may be self-regulated by zonal flows due to the total charge conservation. If this is the case, the fluctuation level associated with the density holes will be controlled, in part, by the collisional damping of zonal flows, $\langle \delta n_{hole}^2 \rangle \propto \nu_d$. Since ν_d typically increases towards the edge, it seems that even with the zonal flow coupling the fluctuation drive by the incoming hole structures becomes increasingly important in "No Man's Land."

At this point it may be appropriate to discuss how we could identify such structures by both physical and digital experiments. On physical experiments, there are of course the measurements of the skewness of density fluctuations by Boedo.[1,2] However, while such experiments show the formation of structures at the tokamak edge, they do not provide a direct evidence of propagating structures in the edge-core coupling region. A possible extension of the experiment by Boedo would be then to combine the skewness plot by Boedo with the Doppler back scattering (DBS) measurement which shows a spatio-temporal evolution of turbulent fluctuations. The simultaneous measurements of the skewness at the edge and the propagating turbulence from the edge will suggest a possible propagation of holes from the edge to the core. Of course, the argument does not show a direct evidence of propagating structures in the core region, since the DBS measurement gives δn^2, which does not distinguish holes ($\delta n < 0$) and blobs ($\delta n > 0$). We might expect such distinction of holes and blobs could be made, for example by electron cyclotron emission imaging (ECEI) measurement which can directly measures δT. However, we note that the ECEI measurement has the resolution of 0.9 cm in the radial direction.[43] Such resolution would not be enough to resolve structures in the edge-core coupling region, with the spatial extent of $\lambda_k \sim \rho_s \sim 0.1$ cm (λ_k is the screening length, ρ_s is the ion sound Larmor radius, and we assumed $T_e \sim 1$ keV and $B \sim 10^4$ Gauss).

In order to identify hole structures by gyrokinetic codes, say electron drift holes discussed in this paper, we would need (i) the parallel nonlinearity in f_e evolution in order to describe the trapping effect in a electrostatic potential and (ii) then a high resolution in the velocity variable to resolve the scale of structures $\Delta v_T \sim \sqrt{|e|\tilde{\phi}/T_e} = v_{the}\sqrt{|e|\tilde{\phi}/T_e}$. The required resolution is roughly estimated as follows. At the level of an order of magnitude estimate, the size of structures is given by $\Delta v_T \sim 3 \times 10^{-2} \times v_{the}$, where the fluctuation amplitude is estimated by the mixing length theory:

$$\frac{|e|\tilde{\phi}}{T_e} \sim \frac{1}{k_\perp L_n} \sim \frac{\rho_s}{L_n} \sim \frac{0.1\,\text{cm}}{100\,\text{cm}} \sim 10^{-3}. \qquad (57)$$
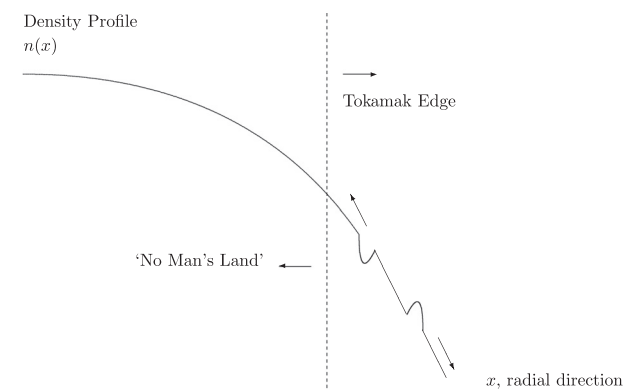
Then, if a simulation covers the velocity space of a few thermal velocity, such as $-5v_{the} < v_\parallel < 5v_{the}$, we need a resolution (here we measure a resolution by points in a simulation domain) of the order of 10^3. Indeed, such high resolution of the velocity space of the order of 10^3 is utilized in a simulation which identifies phase space structures in the 1D Vlasov turbulence.[10]

The paradigm presented here may be also applied to several other relevant issues, such as (i) anomaly of electron heat transport in the linear ohmic regime with large electron drift velocity,[44] where linear eigenmodes of interest (current driven drift waves) are predicted to be marginal,[45] (ii) intrinsic rotation drive, where structure driven turbulence may leads to a source of residual stress and acts as a heat engine[46] to convert radial inhomogeneity to rotation, and (iii) energetic particle confinement where strong wave-particle resonance is expected.[47] These are pursued in future publications.

ACKNOWLEDGMENTS

APPENDIX: MAXWELL-BOLTZMANN HOLE AND AXISYMMETRIC SOLUTION

The axisymmetric ($\partial_y = 0$) solution of the GK Poisson equation with the Maxwell-Boltzmann hole is analyzed. This solution physically describes an anisotropic $E \times B$ vortex extended in y direction. As such, the solution so obtained may be viewed as a "zonal"; however, we note that a finite $k_\parallel \neq 0$ is required for a non-trivial parallel dynamics, including adiabatic electron response as well as electron trapping. Given the caveat, we refer the axisymmetric solution as the "quasi"-zonal hole. Now, the axisymmetric condition $\partial_y = 0$ reduces the GK Poisson equation to a (1D) problem by reducing the screening length to

$$\hat{\lambda}^{-2} = \rho_s^{-2}. \tag{A1}$$

In this case, the screening is determined solely by adiabatic electrons. Note the screening feedback of zonal flow is absent here. Now, to proceed further, we also assume a small hole $(E + |e|\phi_m)/\tau \ll 1$. In this case, the GK Poisson equation reduces to a 1D, albeit nonlinear, equation

$$\partial_x^2 \frac{|e|\phi}{T_e} - \frac{1}{\rho_s^2}\frac{|e|\phi}{T_e} \cong -\frac{1}{\rho_s^2}\frac{4\sqrt{2}}{3}\langle f_e\rangle_0 v_{the}\frac{T_e}{\tau}\left(\frac{|e|\phi}{T_e} - \frac{|e|\phi_m}{T_e}\right)^{3/2}. \tag{A2}$$

With dimensionless variables

$$w \equiv \left(\frac{16\sqrt{2}}{15}\langle f_e\rangle_0 v_{the}\frac{T_e}{\tau}\right)^2\frac{|e|\phi}{T_e}, \quad \xi \equiv \frac{x}{\rho_s}. \tag{A3}$$

we have

$$\partial_\xi^2 w - w + \frac{5}{4}(w - w_m)^{3/2} = 0. \tag{A4}$$

We seek for a localized solution with $w, \partial_\xi w \to 0$ as $\xi \to \pm\infty$. We also set $w_m = 0$ hereafter, which fix the trapping energy to zero (i.e., $E < -|e|\phi_m = 0$ for trapping). Interestingly, Eq. (A4) can be viewed as the equation of motion for a point particle with nonlinear spring constant. The analogy is clear if we take ξ as time and w as a displacement. Then, we can see that Eq. (A4) is the equation of motion with the nonlinear spring constant $1 - 5/4w^{1/2}$. To gain an insight into the "trajectory" produced by Eq. (A4), it is useful to note "energy" is conserved

$$\frac{\partial}{\partial\xi}\left[\frac{1}{2}\left(\frac{\partial w}{\partial\xi}\right)^2 - \frac{1}{2}w^2 + \frac{1}{2}w^{5/2}\right] = 0 \tag{A5}$$

or

$$\left(\frac{\partial w}{\partial\xi}\right)^2 + V(w) = 0, \tag{A6}$$

where $V(w) = -w^2 + w^{5/2}$ is the Sagdeev potential.[48] $V(w)$ is plotted in Fig. 11. From the figure, we can see that $V(w)$ has a trough which allows a localized, bound solution for the electrostatic potential w. The solution is obtained via quadrature as follows. The energy conservation yields

$$\xi = \pm\int_{w_0}^w \frac{dw'}{\sqrt{w'^2 - w'^{5/2}}}, \tag{A7}$$

where w_0 is the value of potential at $\xi = 0$, which is a maximum and $w_0 = 1$ from Fig. 11. The integral can be performed by setting $w' = \sin^4\theta'$, leading to

$$w = \text{sech}^4\left(\frac{\xi}{4}\right). \tag{A8}$$
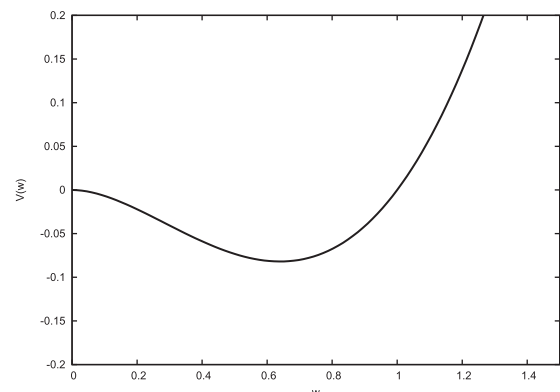
FIG. 11. Sagdeev Potential $V(w)$.

The quasi-zonal solution w is a localized potential in x, with the spatial extent of $\sim 4\rho_s$. Note $w > 0$, which is amenable to electron trapping. By its construction, Eq. (A8) can be thought of as a soliton solution of GK-Poisson system, while it differs from usual solitons, such as ion acoustic solitons, in that the amplitude and the spatial extent is independent.

[1] J. A. Boedo, D. Rudakov, R. Moyer, S. Krasheninnikov, D. Whyte, G. McKee, G. Tynan, M. Schaffer, P. Stangeby, P. West, S. Allen, T. Evans, R. Fonck, E. Hollmann, A. Lenard, A. Mahdavi, G. Porter, M. Tillack, and G. Antar, Phys. Plasmas **8**, 4826 (2001).

[2] J. A. Boedo, D. L. Rudakov, R. A. Moyer, G. R. McKee, R. J. Colchin, M. J. Schaffer, P. G. Stangeby, W. P. West, S. L. Allen, T. E. Evans, R. J. Fonck, E. M. Hollmann, S. Krasheninnikov, A. W. Leonard, W. Nevins, M. A. Mahdavi, G. D. Porter, G. R. Tynan, D. G. White, and X. Xu, Phys. Plasmas **10**, 1670 (2003).

[3] I. B. Bernstein, J. M. Greene, and M. D. Kruskal, Phys. Rev. **108**, 546 (1957).

[4] T. H. Dupree, Phys. Fluids **25**, 277 (1982).

[5] H. L. Berk, B. N. Breizman, and M. Pekker, Phys. Plasmas **2**, 3007 (1995).

[6] T. H. Dupree, Phys. Fluids **26**, 2460 (1983).

[7] R. H. Berman, D. J. Tetreault, and T. H. Dupree, Phys. Fluids **28**, 155 (1985).

[8] R. H. Berman, T. H. Dupree, and D. J. Tetreault, Phys. Fluids **29**, 2860 (1986).

[9] M. Lesur, Y. Idomura, K. Shinohara, X. Garbet, and the JT-60 Team, Phys. Plasmas **17**, 122311 (2010).

[10] M. Lesur, Y. Idomura, and X. Garbet, Phys. Plasmas **16**, 092305 (2009).

[11] P. W. Terry, P. H. Diamond, and T. S. Hahm, Phys. Fluids B **2**, 2048 (1990).

[12] P. H. Diamond, S.-I. Itoh, K. Itoh, and T. S. Hahm, Plasma Phys. Controlled Fusion **47**, R35 (2005).

[13] G. I. Taylor, Philos. Trans. R. Soc. London, Ser. A **215**, 1 (1915).

[14] P. H. Diamond, O. D. Gurcan, T. S. Hahm, K. Miki, Y. Kosuga, and X. Garbet, Plasma Phys. Controlled Fusion **50**, 124018 (2008).

[15] P. H. Diamond and Y.-B. Kim, Phys. Fluids B **3**, 1626 (1991).

[16] P. H. Diamond, A. Hasegawa, and K. Mima, Plasma Phys. Controlled Fusion **53**, 124001 (2011).

[17] A. Hasegawa and M. Wakatani, Phys. Rev. Lett. **50**, 682 (1983).

[18] J. G. Charney and P. G. Drazin, J. Geophys. Res. **66**, 83, doi: 10.1029/JZ066i001p00083 (1961).

[19] B. A. Carreras, K. Sidikman, P. H. Diamond, P. W. Terry, and L. Garcia, Phys. Fluids B **4**, 3115 (1992).

[20] L. D. Pearlstein and H. L. Berk, Phys. Rev. Lett. **23**, 220 (1969).

[21] P. H. Diamond, Y.-M. Liang, B. A. Carreras, and P. W. Terry, Phys. Rev. Lett. **72**, 2565 (1994).

[22] A. Hasegawa, C. G. Maclennan, and Y. Kodama, Phys. Fluids **22**, 2122 (1979).

[23] P. B. Rhines and W. R. Holland, Dyn. Atmos. Oceans **3**, 289 (1979).

[24] T. S. Hahm, Phys. Fluids **31**, 1940 (1988).

[25] A. J. Brizard and T. S. Hahm, Rev. Mod. Phys. **79**, 421 (2007).

[26] P. G. Drazin and W. H. Reid, *Hydrodynamic Stability* (Cambridge University Press, Cambridge, 2004).

[27] L. D. Landau and E. M. Lifshitz, *Quantum Mechanics (Non-Relativistic Theory): Course of Theoretical Physics* (Butterworth-Heinemann, Oxford, 1977), Vol. 3.

[28] C. J. McDevitt, P. H. Diamond, O. D. Gurcan, and T. S. Hahm, Phys. Plasmas **16**, 052302 (2009).

[29] C. J. McDevitt, P. H. Diamond, O. D. Gurcan, and T. S. Hahm, Phys. Rev. Lett. **103**, 205003 (2009).

[30] D. G. Andrew and M. E. McIntyre, J. Fluid Mech. **89**, 647 (1978).

[31] P. H. Diamond, S.-I. Itoh, and K. Itoh, *Modern Plasma Physics: Physical Kinetics of Turbulent Plasmas* (Cambridge University Press, Cambridge, 2011), Vol. 1.

[32] Y. Kosuga and P. H. Diamond, Plasma Fusion Res. **5**, S2051 (2010).

[33] J. Binney and S. Tremaine, *Galactic Dynamics* (Princeton University, Princeton, 2008).

[34] L. A. Charlton, B. A. Carreras, V. E. Lynch, K. L. Sidikman, and P. H. Diamond, Phys. Plasmas **1**, 2700 (1994).

[35] B. N. Rogers, W. Dorland, and M. Kotschenreuther, Phys. Rev. Lett. **85**, 5336 (2000).

[36] S. Champeaux and P. H. Diamond, Phys. Lett. A **288**, 214 (2001).

[37] Z. Guo, L. Chen, and F. Zonca, Phys. Rev. Lett. **103**, 055002 (2009).

[38] Y. Kosuga and P. H. Diamond, Phys. Plasmas **18**, 122305 (2011).

[39] T. H. Dupree, Phys. Fluids **15**, 334 (1972).

[40] P. H. Diamond, P. L. Similon, P. W. Terry, C. W. Horton, S. M. Mahajan, J. D. Meiss, M. N. Rosenbluth, K. Swartz, T. Tajima, and R. D. Hazeltine, *Plasma Physics and Controlled Nuclear Fusion Research 1982* (IAEA, Vienna, 1983), Vol. 1.

[41] H. Biglari, P. H. Diamond, and P. W. Terry, Phys. Fluids **31**, 2644 (1988).

[42] H. Biglari, P. H. Diamond, and P. W. Terry, Phys. Rev. Lett. **60**, 200 (1987).

[43] L. Yu, C. W. Domier, X. Kong, S. Che, B. Tobias, H. Park, C. X. Yu, and N. C. Luhmann, Jr., JINST **7**, C02055 (2012).

[44] L. Lin, M. Porkolab, E. M. Edlund, J. C. Rost, M. Greenwald, N. Tsujii, J. Candy, R. E. Waltz, and D. R. Mikkelsen, Plasma Phys. Controlled Fusion **51**, 065006 (2009).

[45] M. N. Rosenbluth and C. S. Liu, Phys. Fluids **15**, 1801 (1972).

[46] Y. Kosuga, P. H. Diamond, and O. D. Gurcan, Phys. Plasmas **17**, 102313 (2010).

[47] F. Zonca, S. Briguglio, L. Chen, G. Fogaccia, and G. Vlad, Nucl. Fusion **45**, 477 (2005).

[48] L. P. Pitaevskii and E. M. Lifshitz, *Physical Kinetics: Course of Theoretical Physics* (Pergamon, Oxford, 1981), Vol. 10.